Since January 2020 Elsevier has created a COVID-19 resource centre with free information in English and Mandarin on the novel coronavirus COVID-19. The COVID-19 resource centre is hosted on Elsevier Connect, the company's public news and information website.

Journal of Clinical Virology 165 (2023) 105499

Contents lists available at ScienceDirect

Journal of Clinical Virology

journal homepage: www.elsevier.com/locate/jcv

Comparison of the Ct-values for genomic and subgenomic SARS-CoV-2 RNA reveals limited predictive value for the presence of replication competent virus

Fabian Roesmann [a], Irene Jakobsche [a], Christiane Pallas [a], Alexander Wilhelm [a], Johanna Raffel [a], Niko Kohmer [a], Tuna Toptan [a], Annemarie Berger [a], Udo Goetsch [b], Sandra Ciesek [a,c,d], Marek Widera [a,*]

[a] Institute for Medical Virology, University Hospital Frankfurt, Goethe University Frankfurt am Main, Sandhofstr. 2-4, House 75, Room 1.207, Frankfurt am Main 60528, Germany
[b] Health Protection Authority, Frankfurt am Main, Germany
[c] German Center for Infection Research, DZIF, Braunschweig, Germany
[d] Branch Translational Medicine and Pharmacology, Fraunhofer Institute for Molecular Biology and Applied Ecology (IME), Frankfurt am Main, Germany

ARTICLE INFO

Keywords:
SARS-CoV-2
Genomic RNA
Subgenomic RNA
Viral culture
Infectivity

ABSTRACT

SARS-CoV-2 is the causative agent of the acute respiratory disease COVID-19. In addition to the full length positive-sensed, single-stranded genomic RNA (gRNA), viral subgenomic RNAs (sgRNAs) that are required for expression of the 3′ region of the genome are synthesized in virus-infected cells. However, whether these sgRNA-species might be used as a measure of active virus replication and to predict infectivity is still under debate. The commonly used methods to monitor and quantitate SARS-CoV-2 infections are based on RT-qPCR analysis and the detection of gRNA. The infectivity of a sample obtained from nasopharyngeal or throat swabs is associated with the viral load and inversely correlates with Ct-values, however, a cut-off value predicting the infectivity highly depends on the performance of the assay. Furthermore, gRNA derived Ct-values result from nucleic acid detection and do not necessarily correspond to active replicating virus.

We established a multiplex RT-qPCR assay on the cobas 6800 omni utility channel concomitantly detecting SARS-CoV-2 $gRNA_{Orf1a/b}$, $sgRNA_{E,7a,N}$, and human RNaseP-mRNA used as human input control. We compared the target specific Ct-values with the viral culture frequency and performed ROC curve analysis to determine the assay sensitivity and specificity.

We found no advantage in the prediction of viral culture when using sgRNA detection compared to gRNA only, since Ct-values for gRNA and sgRNA were highly correlated and gRNA offered a slightly more reliable predictive value. Single Ct-values alone only provide a very limited prediction for the presence of replication competent virus. Hence, careful consideration of the medical history including symptom onset has to be considered for risk stratification.

1. Introduction

The diagnostic gold-standard for the detection of SARS-CoV-2 infection is the quantitative reverse transcription PCR (RT-qPCR). Commonly, SARS-CoV-2 genomic RNA (gRNA) is detected and it is assumed, that the infectiousness of a SARS-CoV-2 positive individual is correlated with the viral load and thus, inversely correlates with Ct-values [1–3]. However, Ct-values highly depend on the quality of the swab sample. Additionally, Ct-values result from nucleic acid detection alone and might detect fragmented gRNA from defective viral particles. In contrast to replication competent virus, SARS-CoV-2 gRNA is still detectable in RT-qPCR weeks after symptom onset in many convalescent patients [4–6] while viral culture assays remain negative [1,2,7].

The SARS-CoV-2 genomic RNA comprises two large overlapping open reading frames (ORF1a and ORF1b) encoding non-structural proteins (NSPs) that are essential for viral replication and transcription. In

* Corresponding author.
E-mail address: marek.widera@kgu.de (M. Widera).

https://doi.org/10.1016/j.jcv.2023.105499
Received 16 February 2023; Received in revised form 23 May 2023; Accepted 28 May 2023
Available online 29 May 2023

addition, subgenomic RNAs [8] encode the structural proteins spike (S), envelope (E), membrane (M) and nucleocapsid protein (N) and several accessory proteins including 3a, 6, 7a, 7b, 8, and 10 . Since these sgRNAs are exclusively formed during active viral replication, their presence could potentially serve as a surrogate marker for infectiousness. Indeed, multiple studies have shown a correlation between the presence of sgRNA levels and viral culture success in cell culture [7,9–15]. Contradictory, in comparable studies the detection of sgRNA was not a superior biomarker [16–19]. Importantly, many of these studies had limitations as an insufficient limit of detection (LOD) for sgRNA detection, lacking viral culture data, or swab quality controls.

Hence, in this study we established a high performance multiplex RT-qPCR test using the cobas6800 omni-utility-channel (Roche) concomitantly detecting SARS-CoV-2 gRNA, the three most abundant sgRNAs and a spliced human RNaseP to monitor the swab quality. Using this assay, we evaluated whether sgRNA might be a superior surrogate marker to assess the infectivity of a sample.

2. Material and methods

2.1. Study design

From September until December 2020, fresh nasopharyngeal or throat swab samples were collected by the Public Health Department of the City of Frankfurt am Main, Germany. Samples were eluted in 1.5 ml PBS to recover infectious SARS-CoV-2 immediately after arrival in the laboratory. 500 µl of eluted virus suspension was used to infect highly permissive Caco2 cells as described previously [20–22]. 1 ml of the swab dilution was mixed (1:1) with cobas omni lysis reagent (Roche) and subjected to RT-qPCR-analysis using the SARS-CoV-2 Test on the cobas 6800 system, according to manufacturer's instructions (Roche) (Fig. 1). The remaining sample was stored at −20 °C and subjected to multiplex RT-qPCR analysis using the omni-utility-channel (Roche).

2.2. Viral culture

For viral culture, Caco2 cells were used under BSL-3 conditions as described previously [20,21,23]. Supernatant from cells with cytopathic effect (CPE) were subjected to RT-PCR-analysis (M, RdRp) to confirm the SARS-CoV-2 outgrowth as described previously [22,24].

2.3. Diagnostic SARS-CoV-2 RT-qPCR test

The cobas SARS-CoV-2 test (Roche) detecting Orf1a/b and E was used as a qualitative *in vitro* nucleic acid amplification test for the direct detection of SARS-CoV-2 RNA. The assay was performed on the cobas 6800 System (Roche) according to the manufacturer's instructions.

2.4. Multiplex RT-qPCR for simultaneous detection of SARS-CoV-2 gRNA, sgRNA, and RNaseP

Primer and probe sequences (Supp.Table 2) were obtained from Integrated DNA Technologies (IDT). Multiple primer and probes were excessively tested in single versus multiplex PCR-reactions (data not shown) to avoid dimerization issues and to titrate optimal primer probe concentrations (Supp.Table 2). Assay optimization was performed using the cobas omni Optimization Kit (Roche) following the manufacturer's instructions.

One of the primary objectives of this study was the establishment of a high-throughput assay on a diagnostic instrument for the monitoring of active SARS-CoV-2 replication. Therefore, we conducted the cobas 6800 system (Roche) which facilitates a sample-to-answer platform by performing the extraction and PCR reaction autonomously. Additionally, the omni-utility channel of the device allowed us to use the previously optimized primer-probe ratios by loading the cartridges accordingly and to perform RT-qPCR under optimal conditions. The internal control (IC) was included in the test cassette, and all other primers and probes (Supp. Table 2) were added to MMX-R2 reagent and loaded into cobas omni utility channel cassettes (Roche) according to the manufacturer's instructions.

Initial evaluation of the generated primer and probe pairs for the in-house assay was performed on the BioRad CFX96 C1000 5-plex cycler using random samples from routine COVID-19 diagnostics because it is routinely used in the laboratory, allowing multiple adaptations and titrations of the multiplex assay in an easily accessible manner. CAL Fluor Red 635 Calibration Standard (T10) (Biocat, Cat# RD-5084-5-BS) was used to calibrate the BioRad CFX96 C1000 cycler to enable LC640 detection. After optimizing the multiplex assay on the BioRad CFX96, a final validation run had to be performed on an instrument with similar detection machinery to the cobas 6800 system. Therefore, the LightCycler 480 (Roche) was used in the intermediate stage of evaluation. For internal control, the RNA Process Control Kit (Roche, Cat# 07099622001) was used as instructed by the manufacturer. As

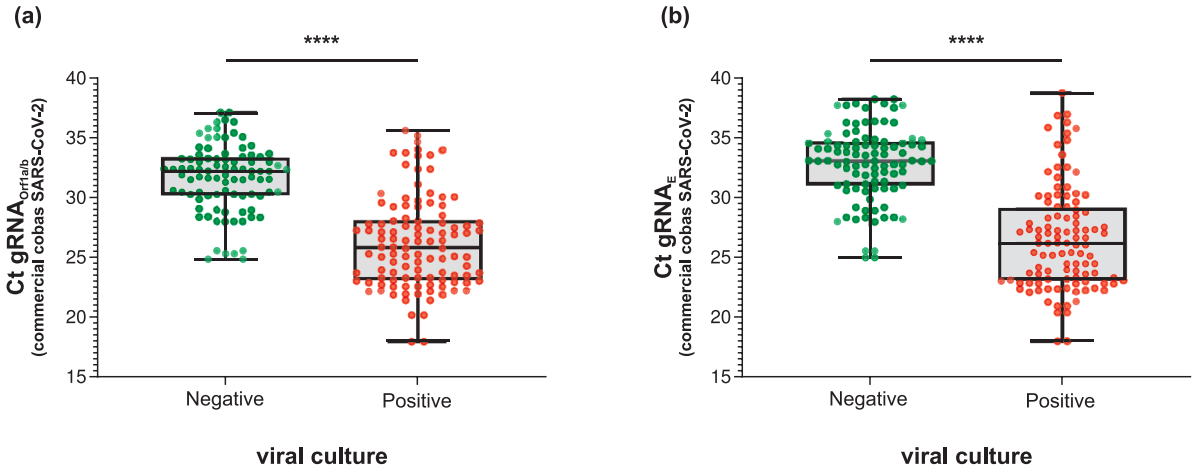

Fig. 1. Correlation between SARS-CoV-2 Ct-values and viral culture. Ct-values were obtained from testing on the cobas 6800 system using the SARS-CoV-2 Test (Roche) targeting SARS-CoV-2 Orf1a/b and E genes. Viral culture assays were performed on Caco2 cells and monitored over a period of 7 days after inoculation. If no CPE was visible after 7 days the sample was deemed negative. Box plots of the (a) Ct_{gRNA} (Orf1a/b) and (b) Ct_{gRNA} (E) values subdivided depending on viral culture (green = negative, red = positive). Whiskers indicating minimum and maximum values. A two-tailed *t*-test was performed to evaluate statistical significance. Asterisks indicate p-values as * ($p < 0.05$), ** ($p < 0.01$), *** ($p < 0.001$) and **** ($p < 0.0001$). Undetected samples were excluded from analyses.

previously described [25] glyceraldehyde-3-phosphate dehydrogenase (GAPDH) mRNA was used as an additional housekeeping gene.

All Ct-values measured within the specified number of cycles were considered as detected (Supp.Table 1).

2.5. Data analysis and software

Cobas 6800 software version 1.4.7.1003 and cobas omni Utility Channel software 3.0 was used in this study. For data performed on BioRad CFX96 device, BioRad Maestro software version 2.3 was used. The software version 1.5.1.62 was used for experiments performed in the LightCycler 480 (Roche).

2.6. Statistical analysis

Figures and statistical analysis were generated with GraphPad Prism (version 9.5.0, GraphPad Software, LLC). ROC curves were generated using MedCalc statistical software version 15.8. Statistical differences between the groups was calculated as indicated in each figure legend.

3. Results

3.1. Comparison of RT-qPCR-derived Ct-values with infectivity in cell culture reveals only a limited predictive value for the presence of replication competent SARS-CoV-2

A total of 267 nasopharyngeal or throat swab samples were detected as SARS-CoV-2 positive by the commercial assay. Subsequently, 110 positive samples were subjected to the viral culture assay. From 104 isolates RNA was recovered and subjected to full-genome sequence analysis (Illumina Next-Generation-Sequencing) showing a wide distribution and variety of SARS-CoV-2 variants including B.1.177, B.1.160, B.1.1.70, B.1.221, and other including variant of concern Alpha (B.1.1.7) as published elsewhere [22]. The median Ct-value of cell culture positive samples was $24.3_{(Orf1a/b)}$ and $24.4_{(E)}$ respectively, while the median Ct-value of cell culture negative samples was $31.7_{(Orf1a/b)}$ and $33.8_{(E)}$. The highest Ct-value of samples with positive outgrowth was $35.6_{(Orf1a/b)}$ and $38.7_{(E)}$. We found that no clear discrimination between cell culture positive and negative samples could be observed indicating that single Ct-values alone only provide a very limited prediction for the presence of replication competent virus. Hence, an assay detecting direct infectivity is needed in order to predict viral culture growth success.

3.2. Development of a SARS-CoV-2 RT-qPCR multiplex assay for the detection of gRNA, sgRNA and a human input control as a possible prediction for viral culture success

In this study we developed an in-house RT-qPCR multiplex assay for the concomitant detection of SARS-CoV-2 gRNA (Orf1a/b), the most abundant SARS-CoV-2 sgRNAs (7a,E,N) and a spliced human input control (RNaseP) to be performed on the cobas 6800 and the Omni Utility channel (Roche Diagnostics). For the detection of viral gRNA, primers and a probe matching Orf1a/b were designed covering nucleotide positions 11.980 to 12.087 in the Orf1a/b open reading frame (Supp.Table 2).

Since the viral RNA leader serves as a starting point for subgenomic transcription during SARS-CoV-2 replication, creating mRNA isoform sequence-specific junctions, we designed primer and probe sets (Supp. Table 2) covering these unique junctions (Fig. 2) previously identified by NGS sequencing of SARS-CoV-2 infected Caco2 cells (data not shown). For validation of the multiplex assay a plasmid was used as template in the RT-qPCR reactions. The plasmid codes for the RNaseP (human input control), $gRNA_{(Orf1a/b)}$, and the three most abundant SARS-CoV-2 $sgRNAs_{(7a,E,N)}$. The binding sites of each primer and probe are visualized in Supplementary Fig. 2.

An universal forward primer and probe was used for the detection of all analyzed sgRNAs [26]. Reverse primer sets targeting the three most abundant sgRNAs 7a, E, and N (Supp.Table 2) were designed for the amplification of all sgRNA products and concomitant detection in the HEX channel (Supp.Table 2, Fig. 2). As human input control we included a primer/probe set for the detection of the low abundant RNaseP, which correlated well to GAPDH mRNA levels (Supp.Fig. 3).

To verify that the assay was also capable of detecting recent SARS-CoV-2 variants including Delta and Omicron, we infected A549-AT cells and isolated the cellular and viral RNA after 6, 12, and 24 h post infection (Supp.Fig. 7). The gRNA and sgRNAs of all tested variants could be detected without loss of sensitivity and were detectable at the earliest 6 h after infection consistent with previously published data [23].

Next, we performed RT-qPCRs of randomly chosen SARS-CoV-2 positive swab samples with a standard qPCR instrument (Fig. 3). The generated Ct-values from the in-house assay were compared with those obtained from the routine diagnostic test performed using the commercial SARS-CoV-2 test. For better comparability with the in-house assay, $Ct_{Orf1a/b}$ was chosen as reference gene.

We obtained a high correlation when comparing the Ct-values (gRNA and sgRNA) with the commercial test (Fig. 3a). The Ct_{RNaseP}-values did not correlate with SARS-CoV-2 RNA levels.

The intra assay Ct-value comparison (Supp.Fig. 5a) revealed a remarkable correlation between SARS-CoV-2 gRNA and sgRNA detection in the multiplex assay. A comparison of RNaseP normalized Ct-values revealed a more heterogeneously distribution of relative viral loads when compared to non-normalized Ct-values alone, indicating relevant differences in sampling quality. However, this normalized appearance did not allow for a clear cut-off between two states. Calculating the $\Delta\Delta Ct_{sgRNA/gRNA}$ by the Livak method [27] subtracting the ΔCt_{gRNA} from the ΔCt_{sgRNA} confirmed a strong RNaseP-dependent dispersion of the relative viral loads values.

In the intermediate state, after initial assessment of the in-house assay, we evaluated the multiplex RT-qPCR on a LightCycler480 (Roche), a PCR machine technically comparable to the cobas 6800

Fig. 2. SARS-CoV-2 sgRNA used for primer and probe design. SARS-CoV-2 leader RNA (excerpt) is shown in black. Coding sequences (CDS, excerpts) are indicated in red. Sequences exclusively present in sgRNA are printed in gray. SARS-CoV-2 RNA species in each line are labeled on the left. The vertical line shown in the middle indicates the sgRNA junction. The respective primer and probe binding sequences are highlighted in bold. Nucleotide positions according to SARS-CoV- 2 reference genome Wuhan-Hu-1 (NC_045512.2).

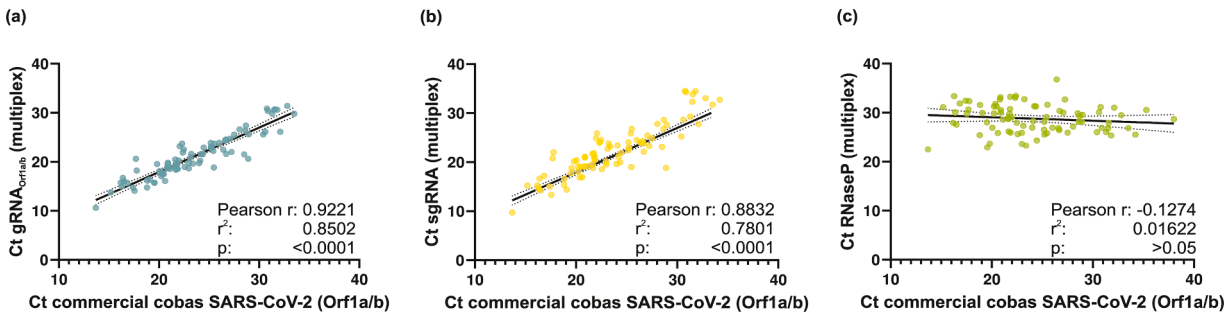

Fig. 3. Correlation of Ct values between in-house SARS-CoV-2 multiplex (y-axis) and commercial Cobas RT-qPCR assays (x-axis). (a) SARS-CoV-2 gRNA (Orf1a/b), (b) SARS-CoV-2 sgRNAs, and (c) RNaseP from spliced human RNA. The Ct-values of the multiplex approach are plotted against the Ct-values obtained from the commercial diagnostic assay performed with the SARS-CoV-2 Test (Roche). The solid line represents the best fit regression line, with the dotted line indicating the 95% CI. Pearson index (r), coefficient of correlation (r2) and significance (p) are indicated. Undetected samples were excluded from analyses.

detection unit. As an internal control and for monitoring the RT efficiency an RNA processing control (Process Control Kit, Roche) was included to exclude possible cross-talks within the multiplex approach. The excellent Pearson index for gRNA (1.00) and sgRNA (0.98) confirmed unbiased performance on both devices, even including the internal control (Supp.Fig. 7).

Next, we implemented the in-house multiplex assay on the cobas 6800 omni-utility-channel and evaluated the performance. Initially we assessed the linearity of the assay (Fig. 4) by serially diluting plasmid-DNA containing all relevant target sequences (Supp.Fig. 2), and spiked a pool of clinical swab samples previously tested negative for SARS-CoV-2 during routine diagnostics. The assay had an excellent signal to noise ratio as shown in the fluorescence curve for each of the SARS-CoV-2 RT-qPCRs (Supp.Fig. 1) and revealed high linearity for all targets (Cts 22–47).

3.3. Evaluation of SARS-CoV-2 subgenomic RNA as a surrogate marker of infectivity

We compared the Ct-values generated by the in-house multiplex assay on the cobas 6800 system (Roche) with the data from the viral culture assay (Fig. 5) and categorized the samples according to positive or negative viral culture. The median Cts detecting SARS-CoV-2 RNAs differed by 10.14 Cts for gRNA and 10.09 for sgRNA between positive and negative samples. The median Ct_{RNaseP} was 36.8 for negative and 39.2 for positive viral culture samples, indicating comparable swab qualities between the groups (Table 1). As expected, positive outgrowth samples overall had lower Ct-values when compared to negative samples (Supp.Table 3).

A comparison of gRNA with sgRNA values, however, revealed a very high correlation with a Pearson index of 0.95, thus only a limited predictive value for the presence of replication competent virus (Fig. 6). This observation was in agreement with previous studies [18] showing that sgRNA copy numbers are dependent on copy number of total SARS-CoV-2 RNA.

A strong correlation of gRNA and sgRNA was observed (Pearson index of 0.95) while both SARS-CoV-2 markers were distinct from the human input control (gRNA/RNaseP and sgRNA/RNaseP) (Fig. 6). This correlation was pronounced when comparing Ct_{gRNA} grouped by detected and undetected sgRNAs (Fig. 7a). Almost all samples with undetectable sgRNA had high Cts_{gRNA} (>30) and no viral culture was observed.

Two samples with Ct_{gRNA}>33 were positive for viral culture, compared to 84 negative ones (data not shown). Analogous the lowest Ct_{gRNA} undetected sgRNA sample had a value of 33.2.

The detection of the sgRNA did not provide any significant advantage in the prediction of viral culture success, only a difference of 3 Cts was observed proportional to the Ct-values. When normalizing Ct_{sgRNA} by 3 Cts the median was almost identical (± 0.025 Ct). A comparison of RNaseP normalized Ct-values as determined by the ΔΔCt-method [27] as described above did not allow for a clear cut-off between positive or negative viral culture (Fig. 7b).

To measure the performance of the multiplex approach as a potential diagnostic test we performed a receiver operating characteristic (ROC) curve analysis. For both gRNA and sgRNA, the areas under ROC curves were highly comparable (Fig. 8). We determined the cutoff points for the prediction of viral culture at Ct_{gRNA} ≤29.97 and Ct_{sgRNA} ≤32.32. Comparing RNaseP normalized ΔCt-values of both parameters ($gRNA_{RNaseP}$ and $sgRNA_{RNaseP}$), we found that the areas under ROC curves were less accurate compared with non-normalized Ct-values. Hence, RNaseP normalization had no advantage in predicting the outgrowth probability in cell culture.

4. Discussion

The aim of this study was to evaluate an RT-qPCR multiplex assay for

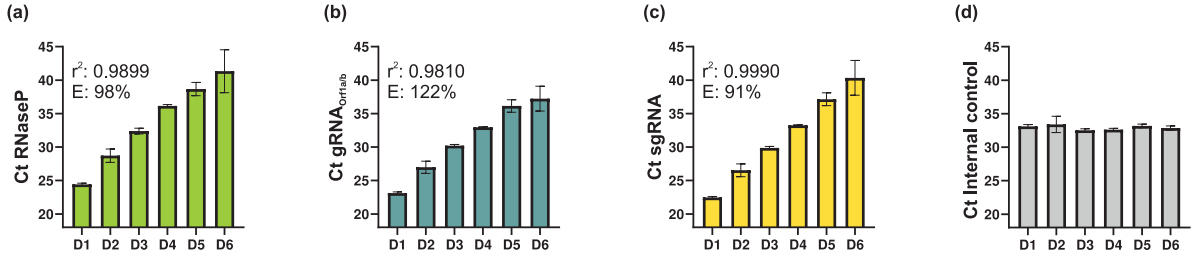

Fig. 4. Determination of the assay linearity. For validation of the in-house multiplex assay using spiked clinical samples tested negative for SARS-Cov-2, a plasmid was used as template in the RT-qPCR reaction. The plasmid codes for the RNaseP (loading control), Orf1 Roche target (gRNA), and the three most abundant SARS-CoV-2 sgRNAs (7a,E,N). (a) Ct_{RNaseP} (b) $Ct_{Orf1a/b}$, (c) Ct_{sgRNA},(d) $Ct_{internal\ control}$ obtained from RT-qPCRs performed with 10-fold serial dilutions (D1-D6) of the calibration plasmid. The assay was performed on the cobas 6800 system in multiple replicates ($n = 5$). Coefficient of determination (R^2) and primer efficiency (E) are indicated.

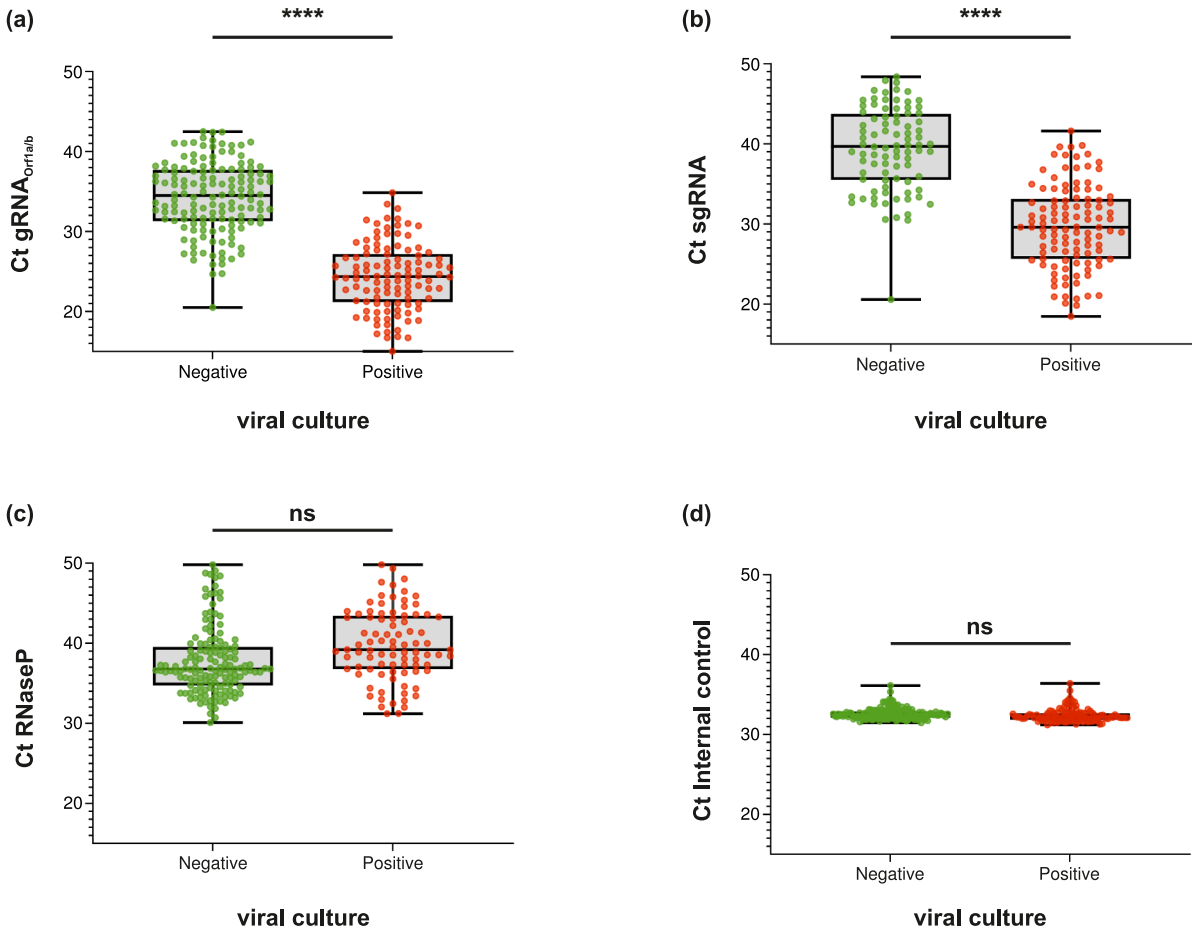

Fig. 5. Correlation between SARS-CoV-2 Ct-values for genomic RNA, sgRNA, RNaseP and viral culture. Ct-values of the in-house multiplex sgRNA assay on the omni Utility Channel on the Roche cobas 6800 device. Ct_{gRNA} (Orf1a/b), Ct_{sgRNA} (E,N,7a), Ct_{RNaseP}, $Ct_{internal\ control}$ is plotted individually for samples positive (red) or negative (green) for SARS-CoV-2 viral culture assay. A two-tailed *t*-test was performed to evaluate statistical significance. Asterisks indicate p-values as * ($p < 0.05$), ** ($p < 0.01$), *** ($p < 0.001$) and **** ($p < 0.0001$). Undetected samples were excluded from analyses.

Table 1
Comparative association of gRNA, sgRNA, RT-PCR detection and viral culture assay. The amount of positive and negative detected RT-PCR samples with gRNA and sgRNA as targets is shown under "RT-PCR detection", with the fraction of samples shown in percent in brackets. A sample was termed negative, if the fluorescence signal did not exceed the background intensity, thus resulting in no cycle threshold. The number of cytopathic effects (CPEs) of the viral culture assays is given, including the fractions shown in percent. The median and interquartile range of the Ct-values of the positive and negative viral culture assays is given under "viral culture". Undetected sgRNA samples were excluded from analyses.

Parameter	Total	negative	Positive	Total	negative	Positive
			RT-PCR detection			
	Orf1a/b (gRNA)			E (gRNA)		
Total no. (%) commerical test	267 (100)	20 (7.5)	247 (92.5)	267 (100)	20 (7.5)	247 (92.5)
	Orf1a/b (gRNA)			E, 7a, N (sgRNA)		
Total no. (%) in-house cobas 6800 Multiplex assay	267 (100)	13 (4.9)	254 (95.1)	267 (100)	70 (26.2)	197 (73.8)
			Viral culture			
CPE (n)	267 (100)	157 (58.8)	110 (41.2)			
			Ct-values in viral culture samples			
	Orf1a/b (gRNA)			E (gRNA)		
Commerical test; Ct	28,9 (24.5; 32,2)	31.7 (29.7; 33.2)	24.3 (21.8; 26.3)	30.0 (25.0; 34.3)	33.8 (31.0; 35.5)	24.4 (21.9; 25.8)
	Orf1a/b (gRNA)			E, 7a, N (sgRNA)		
In-house Cobas 6800 Multiplex assay; Ct	30.4 (24.8; 35.5)	34.5 (31.3; 37.7)	24.4 (21.3; 27.1)	33.4 (29.0; 39.5)	39.7 (35.5; 43.6)	29.6 (26.3; 33.1)

the concomitant detection of SARS-CoV-2 gRNA, sgRNA and a spliced human input control (RNaseP) for the potential suitability as a predictive biomarker for viral culture. A few previously published studies investigated the correlation of sgRNA detection with viral culture as a possible surrogate marker for active viral replication and infectivity, however the conclusions of these studies were in parts contradictory.

An early study by Perera and colleagues reported the detection of sgRNA N at COVID-19 symptom onset, while the copy numbers declined in the following days [9]. Since virus isolation and sgRNA detection were positive within the first 8 days after onset of illness, the authors concluded that patients might be less contagious 8 days after symptom onset. A further study reported detectable sgRNA E transcripts up to 30 days post symptom onset, however, no viral culture assays were performed to correlate sgRNA E detection with infectivity [28].

In another study, the specificity of sgRNA N and S (tested separately) was higher than that of gRNA when compared to viral culture success

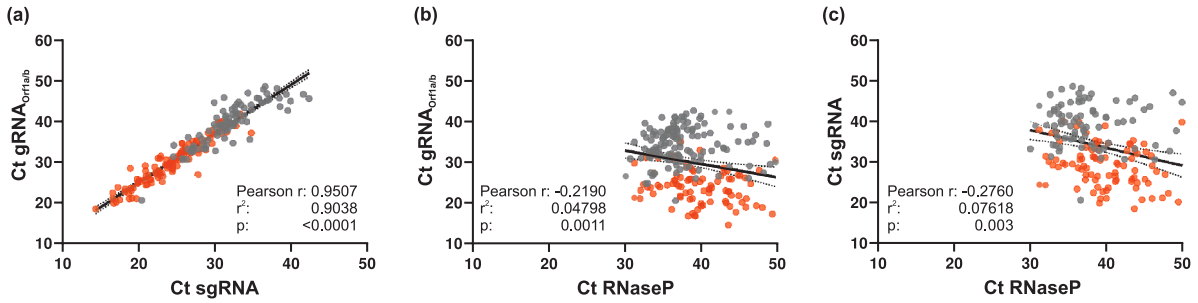

Fig. 6. Correlation between SARS-CoV-2 Ct-values for genomic RNA, sgRNA, RNaseP and viral culture. Ct-values were obtained from testing the samples with the in-house multiplex sgRNA assay on the omni Utility Channel on the Roche cobas 6800 device. (a) Ct_{sgRNA} values against Ct_{gRNA} (Orf1a/b). Ct_{RNaseP} are plotted against (b) $Ct_{Orf1a/b}$ and (c) Ct_{sgRNA} (E,N,7a). Positive (red) and negative (gray) samples of the viral culture assay are indicated. Undetected samples were excluded from analyses.

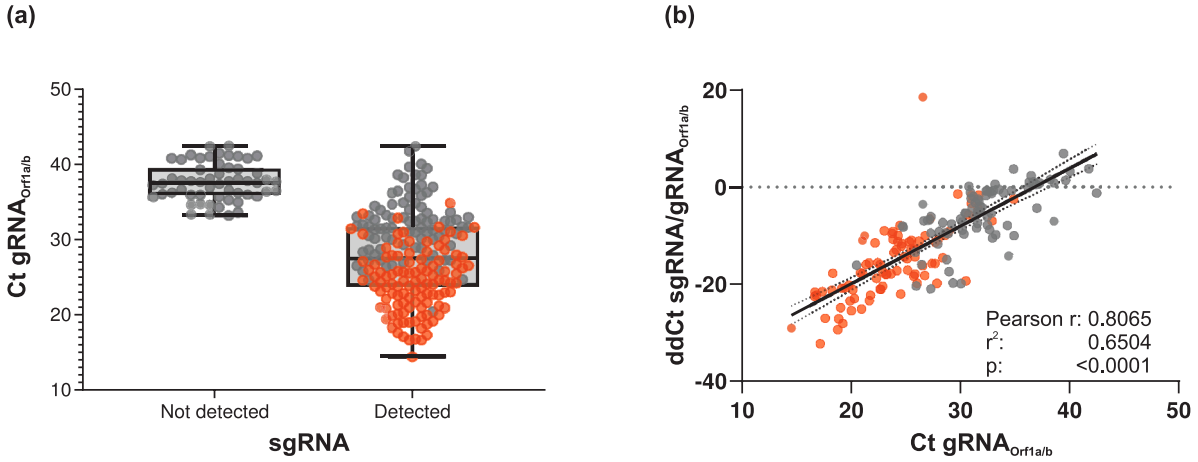

Fig. 7. sgRNA association with gRNA and viral culture. (a) Ct_{gRNA} measured by the in-house cobas 6800 driven multiplex assay of samples with detected and undetected sgRNA. Whiskers indicate minimum and maximum values. (b) Relative RNA abundance was calculated as follows: $\Delta\Delta Ct_{sgRNA\_gRNA}$ (Orf1a/b) = ΔCt_{sgRNA} – ΔCt_{gRNA} (Orf1a/b). The RNaseP normalized expression of gRNA was plotted versus the Ct_{gRNA} values. The solid line indicates the best fit regression line, the 95% CI is illustrated by a dotted line. Positive viral culture samples are highlighted in red, negative samples in gray. Undetected samples were excluded from analyses.

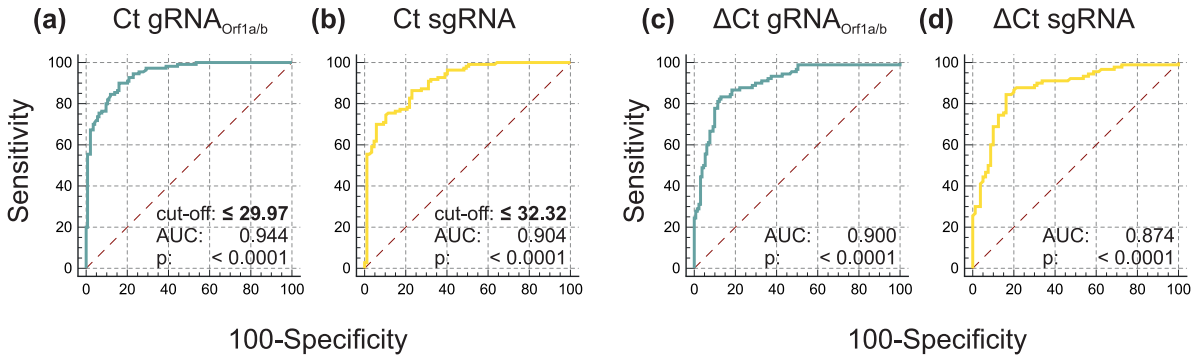

Fig. 8. Receiver operating characteristic (ROC) curves for multiplex RT-qPCR for concomitant SARS-CoV-2 gRNA and sgRNA using human RNaseP normalization. The left panels show the ROC curves resulting from raw Ct-values from SARS-CoV-2 multiplex gRNA and sgRNA detection. The right panels show the ROC curves for RNAseP normalized gRNA and sgRNA expression ($gRNA_{RNaseP}$ and $sgRNA_{RNaseP}$). The cut-off value with the highest sensitivity and specificity is indicated. The area under the curve (AUC) reflects the predictive value i.e. the correct prediction of viral culture, of the analyzed parameter. The p-value shows the likeliness of the parameter to discriminate between positive and negative viral culture. Undetected samples were excluded from analyses.

[11]. Consequently, the authors claimed significant advantage of sgRNA detection in the prediction of infectious material. However, the authors did not correlate the direct Ct-value ratio of gRNA/sgRNA of each sample, which results in a homogenous shift of the Ct distribution of gRNA and sgRNA as seen in our study (Figs. 7 and 5, Table 1). A major limitation of many studies is the limit of detection (LOD) of the respective sgRNA assay. Since it is known, that a cultivation success correlates approximately with a cutoff value of Ct_{gRNA} 30 (depending on the assay) [29] and most likely shifts for sgRNA assays below the LOD, the qualitative statement "detected" or "not detected" might be deceptive. In a large cohort study at a Ct≥30 the outgrowth success dramatically dropped to 20% [29]. This data is in excellent agreement with our results (Figs. 1 and 8) showing an cutoff in cultivation success at $Ct_{SARS\text{-}CoV\text{-}2\text{-}Test}$ 29.7 and Ct_{gRNA} 29.97 (Table 1, Fig. 8). Using a highly

sensitive approach detecting the three most abundant sgRNA species (N, 7a,E) we observed a shift in the cultivation cutoff at Ct_{sgRNA} 32.32. Of note, no viral culture was observed in the absence of sgRNA. In line with this observation, some studies have postulated that the absence of sgRNA results in negative growth success in cell culture, which suggests sgRNA as an advantageous marker [7,9–15]. Our data, however, shows a considerable correlation between Ct_{gRNA} and Ct_{sgRNA} (Fig. 6), and only a shift of 3 Cts (Table 1).

The comparison of the areas determined via ROC curves demonstrated that the detection of the gRNA with the sgRNA was very similar with regard to the predictive capacity for positive virus cultivation and that the Ct-values from both measurement parameters could be compared with each other. However, this also indicates that the SARS-CoV-2 sgRNA does not add any significant value to the prediction performance. In the cohort studied here under optimal conditions, we were able to determine a predictive cut-off value of Ct_{gRNA} of $\leq$29.97 for Ct_{sgRNA} of $\leq$32.32, which corresponds to a difference of 2.35 Ct-values. Comparison with RNaseP-normalized expression values used to match the human input and sampling quality, did not provide any advantage in terms of positive-negative discrimination.

5. Conclusions

Using the novel multiplex assay established in this study, we yield excellent performance and are therefore able to detect low viral loads. This advantage underlines that sgRNA is significantly correlated to the gRNA albeit with an average ΔCt of 3 ($p < 0.0001$; two-tailed *t*-test). Since gRNA was more reliable detected than sgRNA, and yielded a better predictive value shown by the ROC analysis, we conclude, that detection of sgRNA offers no added value in viral culture prediction than detection of gRNA alone. In a multifactorial clinical setting, detection of viral loads by RT-qPCR alone offer only a limited predictive value. A larger cohort analysis would be necessary to provide a conclusive statement on the benefit of sgRNA for predicting the infectivity of patients in a clinical context, including other clinical parameters such as antibody status and titer, HLA, disease severity, immunocompromised status and days since symptom onset [19].

6. Limitations of the study

This study has important limitations: We solely collected nasopharyngeal or throat swabs, to which we did not link to the patient and demographic data. In addition, since randomized samples were analyzed with focus on Ct-values and viral culture success, our data lacks clinical information on COVID-19 severity and associated symptoms.

It has been shown that antibodies correlate with viral culture probability [19]. Among the study participants of this study, the likelihood of a previous SARS-CoV-2 infection is very low since the samples were obtained early during the pandemic, however, cross species antibodies against other coronaviruses have not been evaluated prior to sampling.

Of note, individuals were not screened for immunodeficiency before being included in our cohort. This might be relevant, since immunocompromised patients could have prolonged shedding of infective SARS-CoV-2 but are unlikely to be represented in this cohort [12,30,31]. Additionally, our patient numbers remain small and larger studies are needed to establish Ct_{sgRNA} criteria that reliably correlate with loss of infectivity.

Although, we used Caco2 cells, that have been previously selected for high permissiveness for SARS-COV-2, we cannot exclude factors limiting viral culture in cell culture. The use of additional highly permissive cell models e.g. based on Vero or A549 [23] cells might help to compare reproducibility of the assay.

Data availability

All sequences are available on GISAID (www.gisaid.org), accession numbers EPI_ISL_1138599- EPI_ISL_1138734 [22]. All relevant data are available from the authors upon request. SARS-CoV-2 isolate sequences are available on GenBank under the following accession numbers: SARS-CoV-2 Delta (FFM-IND8424/2021, GenBank ID: MZ315141) [32], SARS-CoV-2 Omicron BA.1 (FFM-ZAF0396/2021; GenBank ID: OL800703), SARS-CoV-2 Omicron BA.2 (FFM-BA.2-3833/2022; GenBank ID: OM617939) [33], SARS-CoV-2 B FFM1/2020 (GenBank ID: MT358638) [24].

Author contributions

M.W., and S.C. designed the study; M.W. designed the experiments, F.R., J.R., C.P., T.T. and I.J performed experiments; U.G., N.K. and T.T. contributed to study design, patient recruitment, and clinical data acquisition. T.T. investigated the sgRNA leader junctions sequences. A. W. performed statistical analysis. M.W., and S.C. supervised all parts of the study; F.R. and M.W. wrote the manuscript. All authors approved the final version of the manuscript.

Ethics statement

This study was performed according to the guidelines of the Declaration of Helsinki, and approved by the Institutional Review Board of the Ethics Committee of the Faculty of Medicine at Goethe University Frankfurt (21-201, 20-864, and 19-2507).

Funding

This study was supported by Roche. M.W. was supported by the Goethe-Corona-Fond of the Goethe University & University Hospital Frankfurt. Moreover, the work was in part supported by the cluster project ENABLE, the Innovation Center TheraNova, and the LOEWE Priority Program CoroPan funded by the Hessian Ministry for Science and the Arts (HMWK). F.R. and M.W. were supported by the DFG (WI 5086/1-1, SPP1923).

Declaration of Competing Interest

M.W. has received research support from Roche, Qiagen and a speaker's fee from Astra Zeneca. All other authors declare no conflicts of interest, financial or otherwise.

Acknowledgments

We thank Gene Spier and Jingtao Sun, Daniel Jarem, Alison Kutcha from Roche Molecular Diagnostics. We thank Marhild Kortenbusch for excellent technical assistance.

Supplementary materials

Supplementary material associated with this article can be found, in the online version, at doi:10.1016/j.jcv.2023.105499.

References

[1] J. Bullard, K. Dust, D. Funk, J.E. Strong, D. Alexander, L. Garnett, et al., Predicting infectious severe acute respiratory syndrome coronavirus 2 from diagnostic samples, Clin. Infect. Dis. 71 (2020) 2663–2666. : an official publication of the Infectious Diseases Society of America.

[2] A. Singanayagam, M. Patel, A. Charlett, J. Lopez Bernal, V. Saliba, J. Ellis, et al., Duration of infectiousness and correlation with RT-PCR cycle threshold values in cases of COVID-19, England, January to May 2020, Eurosurveillance (2020) 25.

[3] M.M. Arons, K.M. Hatfield, S.C. Reddy, A. Kimball, A. James, J.R. Jacobs, et al., Presymptomatic SARS-CoV-2 infections and transmission in a skilled nursing facility, N. Engl. J. Med. 382 (2020) 2081–2090.

[4] Y. Wu, C. Guo, L. Tang, Z. Hong, J. Zhou, X. Dong, et al., Prolonged presence of SARS-CoV-2 viral RNA in faecal samples, Lancet Gastroenterol. Hepatol. 5 (2020) 434–435.

[5] J.P. Ridgway, N.S. Shah, A.A. Robicsek, Prolonged shedding of severe acute respiratory coronavirus virus 2 (SARS-CoV-2) RNA among patients with coronavirus disease 2019 (COVID-19), Infect. Control Hosp. Epidemiol. 41 (2020) 1235–1236. : the official journal of the Society of Hospital Epidemiologists of America.
[6] C. Mattiuzzi, B.M. Henry, F. Sanchis-Gomar, G. Lippi, SARS-CoV-2 recurrent RNA positivity after recovering from coronavirus disease 2019 (COVID-19): a meta-analysis, Acta Biomed. 91 (2020), e2020014.
[7] R. Wolfel, V.M. Corman, W. Guggemos, M. Seilmaier, S. Zange, M.A. Muller, et al., Virological assessment of hospitalized patients with COVID-2019, Nature 581 (2020) 465–469.
[8] D. Kim, J.Y. Lee, J.S. Yang, J.W. Kim, V.N. Kim, H. Chang, The architecture of SARS-CoV-2 transcriptome, Cell 181 (2020) 914–921, e10.
[9] R. Perera, E. Tso, O.T.Y. Tsang, D.N.C. Tsang, K. Fung, Y.W.Y. Leung, et al., SARS-CoV-2 virus culture and subgenomic RNA for respiratory specimens from patients with mild coronavirus disease, Emerg. Infect. Dis. 26 (2020) 2701–2704.
[10] M. Santos Bravo, C. Berengua, P. Marin, M. Esteban, C. Rodriguez, M. Del Cuerpo, et al., Viral culture confirmed SARS-CoV-2 subgenomic RNA value as a good surrogate marker of infectivity, J. Clin. Microbiol. 60 (2022), e0160921.
[11] J.Y. Kim, J.Y. Bae, S. Bae, H.H. Cha, J.S. Kwon, M.H. Suh, et al., Diagnostic usefulness of subgenomic RNA detection of viable SARS-CoV-2 in patients with COVID-19, Clin. Microbiol. Infect. 28 (2022) 101–106. : the official publication of the European Society of Clinical Microbiology and Infectious Diseases.
[12] T.T. Truong, A. Ryutov, U. Pandey, R. Yee, L. Goldberg, D. Bhojwani, et al., Increased viral variants in children and young adults with impaired humoral immunity and persistent SARS-CoV-2 infection: a consecutive case series, EBioMedicine 67 (2021), 103355.
[13] Z. Chen, R.W.Y. Ng, G. Lui, L. Ling, C. Chow, A.C.M. Yeung, et al., Profiling of SARS-CoV-2 subgenomic RNAs in clinical specimens, Microbiol. Spectr. 10 (2022), e0018222.
[14] A. Phuphuakrat, E. Pasomsub, S. Srichatrapimuk, S. Kirdlarp, A. Suksatu, C. Srisaowakarn, et al., Detectable duration of viable SARS-CoV-2, total and subgenomic SARS-CoV-2 RNA in noncritically Ill COVID-19 patients: a prospective cohort study, Microbiol. Spectr. 10 (2022), e0050322.
[15] G. Dagotto, N.B. Mercado, D.R. Martinez, Y.J. Hou, J.P. Nkolola, R.H. Carnahan, et al., Comparison of Subgenomic and Total RNA in SARS-CoV-2 Challenged Rhesus Macaques, J. Virol. (2021) 95.
[16] S. Alexandersen, A. Chamings, T.R. Bhatta, SARS-CoV-2 genomic and subgenomic RNAs in diagnostic samples are not an indicator of active replication, Nat. Commun. 11 (2020) 6059.
[17] R. Verma, E. Kim, G.J. Martinez-Colon, P. Jagannathan, A. Rustagi, J. Parsonnet, et al., SARS-CoV-2 subgenomic RNA kinetics in longitudinal clinical samples, Open Forum Infect. Dis. 8 (2021) ofab310.
[18] D.E. Dimcheff, A.L. Valesano, K.E. Rumfelt, W.J. Fitzsimmons, C. Blair, C. Mirabelli, et al., Severe Acute Respiratory Syndrome Coronavirus 2 Total and Subgenomic RNA Viral Load in Hospitalized Patients, J. Infect. Dis. 224 (2021) 1287–1293.
[19] J.J.A. van Kampen, D. van de Vijver, P.L.A. Fraaij, B.L. Haagmans, M.M. Lamers, N. Okba, et al., Duration and key determinants of infectious virus shedding in hospitalized patients with coronavirus disease-2019 (COVID-19), Nat. Commun. 12 (2021) 267.
[20] D. Bojkova, K. Klann, B. Koch, M. Widera, D. Krause, S. Ciesek, et al., Proteomics of SARS-CoV-2-infected host cells reveals therapy targets, Nature 583 (2020) 469–472.
[21] J. Cinatl Jr., G. Hoever, B. Morgenstern, W. Preiser, J.U. Vogel, W.K. Hofmann, et al., Infection of cultured intestinal epithelial cells with severe acute respiratory syndrome coronavirus, Cell. Mol. Life Sci. CMLS 61 (2004) 2100–2112.
[22] M. Widera, B. Muhlemann, V.M. Corman, T. Toptan, J. Beheim-Schwarzbach, N. Kohmer, et al., Surveillance of SARS-CoV-2 in Frankfurt am main from October to December 2020 reveals high viral diversity including spike mutation N501Y in B.1.1.70 and B.1.1.7, Microorganisms 9 (2021).
[23] M. Widera, A. Wilhelm, T. Toptan, J.M. Raffel, E. Kowarz, F. Roesmann, et al., Generation of a sleeping beauty transposon-based cellular system for rapid and sensitive screening for compounds and cellular factors limiting SARS-CoV-2 replication, Front. Microbiol. 12 (2021), 701198.
[24] T. Toptan, S. Hoehl, S. Westhaus, D. Bojkova, A. Berger, B. Rotter, et al., Optimized qRT-PCR approach for the detection of intra- and extra-cellular SARS-CoV-2 RNAs, Int. J. Mol. Sci. 21 (2020).
[25] H. Sertznig, F. Roesmann, A. Wilhelm, D. Heininger, B. Bleekmann, C. Elsner, et al., SRSF1 acts as an IFN-I-regulated cellular dependency factor decisively affecting HIV-1 post-integration steps, Front. Immunol. 13 (2022).
[26] S. Long, SARS-CoV-2 Subgenomic RNAs: characterization, utility, and perspectives, Viruses 13 (2021).
[27] K.J. Livak, T.D. Schmittgen, Analysis of relative gene expression data using real-time quantitative PCR and the 2(-Delta Delta C(T)) Method, Methods 25 (2001) 402–408.
[28] C.A. Hogan, C. Huang, M.K. Sahoo, H. Wang, B. Jiang, M. Sibai, et al., Strand-specific reverse transcription PCR for detection of replicating SARS-CoV-2, Emerg. Infect. Dis. 27 (2021) 632–635.
[29] R. Jaafar, S. Aherfi, N. Wurtz, C. Grimaldier, T. Van Hoang, P. Colson, et al., Correlation between 3790 quantitative polymerase chain reaction-positives samples and positive cell cultures, including 1941 severe acute respiratory syndrome coronavirus 2 isolates, Clin. Infect. Dis. 72 (2021) e921. : an official publication of the Infectious Diseases Society of America.
[30] A. Sung, A.L. Bailey, H.B. Stewart, D. McDonald, M.A. Wallace, K. Peacock, et al., Isolation of SARS-CoV-2 in Viral Cell Culture in Immunocompromised Patients With Persistently Positive RT-PCR Results, Front. Cell. Infect. Microbiol. 12 (2022), 804175.
[31] Y. Nakajima, A. Ogai, K. Furukawa, R. Arai, R. Anan, Y. Nakano, et al., Prolonged viral shedding of SARS-CoV-2 in an immunocompromised patient, J. Infect. Chemother. 27 (2021) 387–389. : official journal of the Japan Society of Chemotherapy.
[32] A. Wilhelm, T. Toptan, C. Pallas, T. Wolf, U. Goetsch, R. Gottschalk, et al., Antibody-mediated neutralization of authentic SARS-CoV-2 B.1.617 variants harboring L452R and T478K/E484Q, Viruses 13 (2021). Aug 26; 13 (9):1693. doi: 10.3390/v13091693. PMID: 34578275 PMCID: PMC8473269.
[33] A. Wilhelm, M. Widera, K. Grikscheit, T. Toptan, B. Schenk, C. Pallas, et al., Limited neutralisation of the SARS-CoV-2 Omicron subvariants BA.1 and BA.2 by convalescent and vaccine serum and monoclonal antibodies, EBioMedicine 82 (2022), 104158.